



Mass spectrometry-directed structure elucidation and total synthesis of ultra-long chain (O-acyl)- ω -hydroxy fatty acids^S

Sarah E. Hancock,^{1,*†} Ramesh Ailuri,^{†,§} David L. Marshall,^{**} Simon H. J. Brown,^{†,††} Jennifer T. Saville,^{2,§} Venkateswara R. Narreddula,^{**} Nathan R. Boase,^{§§} Berwyck L. J. Poad,^{**} Adam J. Trevitt,[§] Mark D. P. Willcox,^{***} Michael J. Kelso,^{†,§} Todd W. Mitchell,^{3,*†} and Stephen J. Blanksby^{3,**,§§}

School of Medicine,^{*} Illawarra Health and Medical Research Institute,[†] School of Chemistry,[§] and School of Biological Sciences,^{††} University of Wollongong, Wollongong, New South Wales, Australia; Central Analytical Research Facility, Institute for Future Environments^{**} and School of Chemistry, Physics, and Mechanical Engineering,^{§§} Queensland University of Technology, Brisbane, Queensland, Australia; and School of Optometry and Vision Science,^{***} University of New South Wales, Sydney, New South Wales, Australia

ORCID IDs: 0000-0001-7541-8901 (S.E.H.); 0000-0002-1711-2338 (D.L.M.); 0000-0003-3997-4614 (S.H.J.B.); 0000-0001-5504-237X (V.R.N.); 0000-0001-6077-2609 (N.R.B.); 0000-0002-0420-6116 (B.L.J.P.); 0000-0003-2525-3162 (A.J.T.); 0000-0003-3842-7563 (M.D.P.W.); 0000-0001-7809-6637 (M.J.K.); 0000-0002-1372-9963 (T.W.M.); 0000-0002-8560-756X (S.J.B)

Abstract The (O-acyl)- ω -hydroxy FAs (OAHFAs) comprise an unusual lipid subclass present in the skin, vernix caseosa, and meibomian gland secretions. Although they are structurally related to the general class of FA esters of hydroxy FAs (FAHFAs), the ultra-long chain (30–34 carbons) and the putative ω -substitution of the backbone hydroxy FA suggest that OAHFAs have unique biochemistry. Complete structural elucidation of OAHFAs has been challenging because of their low abundance within complex lipid matrices. Furthermore, because these compounds occur as a mixture of closely related isomers, insufficient spectroscopic data have been obtained to guide structure confirmation by total synthesis. Here, we describe the full molecular structure of ultra-long chain OAHFAs extracted from human meibum by exploiting the gas-phase purification of lipids through multi-stage MS and novel multidimensional ion activation methods. The analysis elucidated sites of unsaturation, the stereochemical configuration of carbon-carbon double bonds, and ester linkage regiochemistry. Such isomer-resolved MS guided the first total synthesis of an ultra-long chain OAHFA, which, in turn, confirmed the structure of the most abundant OAHFA found in human meibum, OAHFA 50:2. The availability of a synthetic OAHFA opens new territory for future investigations into the unique biophysical and biochemical properties of these lipids.—Hancock, S. E., R. Ailuri,

D. L. Marshall, S. H. J. Brown, J. T. Saville, V. R. Narreddula, N. R. Boase, B. L. J. Poad, A. J. Trevitt, M. D. P. Willcox, M. J. Kelso, T. W. Mitchell, and S. J. Blanksby. **Mass spectrometry-directed structure elucidation and total synthesis of ultra-long chain (O-acyl)- ω -hydroxy fatty acids.** *J. Lipid Res.* 2018. 59: 1510–1518.

Supplementary key words tandem mass spectrometry • chemical synthesis • eye • secretion • fatty acid esters of hydroxy fatty acids • meibum

The FA esters of hydroxy FAs (FAHFAs) represent a newly described class of lipid (1, 2). Found in mammalian tissues and serum, FAHFAs are thought to have anti-diabetic and anti-inflammatory properties (1, 3, 4). Their structure is relatively simple, consisting of a FA esterified to a hydroxy FA (HFA) substituted at carbon 5, 7, 8, 9, 10, 11, 12

Abbreviations: AMPP, *N*-(4-aminomethylphenyl)pyridinium; CID, collision-induced dissociation; DHP, dihydropyran; FAHFA, FA esters of hydroxy FA; HFA, hydroxy FA; 4-I-AMPP, 1-(3-(aminomethyl)-4-iodophenyl)pyridin-1-ium; OAHFA, (O-acyl)- ω -hydroxy FA; OzID, ozone-induced dissociation; PD, photodissociation; RDD, radical-directed dissociation; R_f, retention factor; THF, tetrahydrofuran; THP, tetrahydropyran; TsOH, *p*-toluene sulfonic acid; WE, wax ester.

¹Present address of S. E. Hancock: School of Medical Sciences, University of New South Wales, Sydney, Australia.

²Present address of J. T. Saville: Genetics and Molecular Pathology, SA Pathology at Women's and Children's Hospital, Adelaide, South Australia, Australia.

³To whom correspondence should be addressed.

e-mail: toddm@uow.edu.au (T.W.M.);

stephen.blanksby@qut.edu.au (S.J.B.)

^SThe online version of this article (available at <http://www.jlr.org>) contains a supplement.

Copyright © 2018 Hancock et al. Published under exclusive license by The American Society for Biochemistry and Molecular Biology, Inc.

This article is available online at <http://www.jlr.org>

This work was supported by Australian Research Council Grants LPI40100711 (Linkage Program, with industry support from Allegan) and FT110100249 (Future Fellowship Scheme, to T. W. M.) and Queensland University of Technology support from the Central Analytical Research Facility operated by the Institute for Future Environments to S. J. B., V. R. N., N. R. B., B. L. J. P., and D. L. M.; and a Postgraduate Research Award to V. R. N.

Manuscript received 5 May 2018 and in revised form 13 June 2018.

Published, JLR Papers in Press, June 15, 2018

DOI <https://doi.org/10.1194/jlr.M086702>

or 13, with both acyl chains typically 16–18 carbons long and having up to a single degree of unsaturation. A structurally related subclass of lipids, the (*O*-acyl)- ω -HFAs (OAHFAs), differ from FAHFAs in that their HFA is ultra-long, typically around 26–34 carbons in length, and their hydroxy esterification is believed to be solely at the terminal (ω) position. OAHFAs have been detected in the skin (5), in equine sperm (6) and amniotic fluid (7), and in waxy secretions from meibomian glands located within the eyelids (i.e., meibum) that supply the tear film lipid layer (8–10). In the tear film lipid layer, OAHFAs represent one of only two amphipathic categories of lipid ($\sim 4\%$ total lipid) (11) and are thought to promote tear film stability and prevent drying of the ocular surface (12, 13). OAHFAs also exist as components of complex lipids, including cholesteryl esters in meibum (14) and vernix caseosa (15), and acylceramides in the skin (i.e., esterified ω -hydroxyacyl-sphingosine) (5, 16–18). The latter have been shown to have a vital role in forming the skin barrier, with disruption to the gene essential for synthesis leading to death from dehydration in neonatal mice (5, 17, 18). The recent discovery of this family of lipids and the demonstration of their diverse biophysical and biochemical functions drives a need to fully elucidate their molecular structure(s) and derive efficient pathways for their synthesis.

The lipidomes of skin, vernix caseosa, and meibum are highly complex and distinct from other mammalian systems in two respects. First, lipids extracted from these sources comprise mostly neutral classes, including wax esters (WEs), triacylglycerols, diacylglycerols, squalene, cholesteryl esters, and diacylated α,ω -diols (13, 19, 20). Second, the lipid components of these tissues are renowned for containing FAs with noncanonical acyl chain lengths and sites of unsaturation [e.g., sapienic acid, 16:1 (*n*-10), is present in vernix caseosa, skin, and sebaceous secretions] and methyl-branched acyl chains (e.g., *iso*-16:0 and *anteiso*-17:0 within WEs of skin, vernix caseosa, and meibum) (21–23).

This variation in the FA building blocks leads to high molecular complexity and, along with the presence of lipid isomers, makes the conventional natural products approach of purification and spectroscopic interrogation of a single naturally occurring OAHFA extremely challenging. As a result, most of our knowledge regarding the elemental composition of OAHFAs is derived from MS, while information on the fatty acyl and HFA components is gleaned from MS/MS (9). Both measurements, however, are blind to important structural characteristics that inform biochemical function, such as sites of unsaturation, carbon-carbon double bond configuration, hydroxylation regiochemistry, and the presence (or absence) of acyl chain branching. Indeed, tandem mass spectra reported to date almost certainly represent composites of numerous isomeric species. While seemingly subtle, the absence of these structural reference points represents a fundamental knowledge gap that precludes reporting of a unique molecular structure as a specific target for synthesis and prevents further studies enabled by the availability of pure compounds. To overcome this limitation, we have developed a customized suite of MS-based strategies that provide unambiguous structure

determination of OAHFAs extracted from human meibum (24). Specifically, these measurements provide unequivocal assignment of sites of unsaturation and ester moieties, exclude significant contributions from acyl chain branching, and assign stereochemical configuration of carbon-carbon double bonds. These structural insights have informed the first total synthesis of ultra-long chain OAHFAs that affords identical mass spectral fingerprints to the natural product across all modes of analysis.

MATERIALS AND METHODS

Nomenclature

Lipid nomenclature used throughout is based on general literature recommendations (25) and customized to describe the OAHFA structure (26). Briefly, sum composition OAHFAs are described as OAHFA X:Y, where X is the total number of carbons and Y is the number of double bonds. Where the stoichiometry of the FA and HFA chains have been determined, lipids are denoted as OAHFA X₁:Y₁/X₂:Y₂, where X₁:Y₁ defines the number of carbons and the degree of unsaturation in the FA and X₂:Y₂ defines the number of carbons and the degree of unsaturation in the HFA. Where double bond position has been determined, the traditional nomenclature “*n*-*x*” is used, where *x* is double bond position from the methyl or omega (ω) end of each acyl chain. Where ester position is confirmed, the OAHFA X₁:Y₁/*y*-O-X₂:Y₂ nomenclature is used, which is modeled on suggestions by Marshall et al. (26). Herein, *y* defines the ester position relative to carboxylic acid and where *y* = ω , the ester is linked via the terminal carbon of the HFA chain. Where double bond stereochemistry is determined, it is indicated as *cis* (*Z*) or *trans* (*E*), respectively.

Materials

All solvents used for meibum collection were purchased from Ajax Finechem. All solvents used for MS and TLC were purchased as the highest grade available (i.e., HPLC or higher) from VWR International Pty Ltd. (Brisbane, QLD, Australia) and used without further purification. Reagents used for OAHFA synthesis, glass-backed silica 60 gel TLC plates, ammonium acetate, and butylated hydroxytoluene were obtained from Sigma-Aldrich Pty Ltd. (Sydney, NSW, Australia). Oleoyl stearate WE (WE 18:1/18:0) standard was purchased from Nu-Chek Prep Inc. (Elysian, MN). The Cayman AMP⁺ MS kit was obtained from Sapphire Bioscience (Sydney, NSW, Australia).

Meibum collection

This study was conducted in compliance with the tenets of the Declaration of Helsinki (2013) and was approved by the University of New South Wales Human Research Ethics Advisory Panel (HC15609). Meibum samples were collected from 10 participants aged between 20 and 30 years. No topical anesthesia was used during meibum collection. None of the participants had any complaint of dry eye; lid margin abnormalities and normal meibum expression was confirmed by observing the expulsion of clear fluid from the meibomian gland orifices following mild digital pressure. The meibomian gland evaluator (TearScience, Morrisville, NC) was used to express the glands on the lower eyelid by gently pressing the evaluator for approximately 10 s throughout the lid below the lash line. A stainless steel ethanol-cleaned and heat-sterilized spatula (ProSciTech, Kirwan, QLD, Australia) was used to collect the expressed meibum by gently sliding across the orifices. The meibum was collected from the lower lids of the participants with particular attention given to avoiding scratching of

the lid margin and contamination with lid epithelial cells and tears. Meibum collected on the spatula was placed in a glass vial (ProSciTech) containing 1 ml of chloroform and stirred until completely dissolved. The vial was capped immediately and stored at -80°C until used for analysis. Prior to analysis, meibum was transferred to a sleeved glass vial, dried under N_2 , and resuspended in 200 μl of chloroform.

OAHFA purification

An enriched OAHFA extract was prepared from meibum by TLC. Each meibum sample was deposited dropwise by glass capillary onto a Silica Gel 60 TLC plate alongside a 0.7 $\text{mg}\cdot\text{ml}^{-1}$ mixture of WE 18:1/18:0, OAHFA 18:1 (*n*-9, *cis*)/ ω -O-16:0 and OAHFA 18:1 (*n*-9, *cis*)/ ω -O-32:1 (*n*-7, *cis*) **2** standards (1:1:1 w/v). Each drop was allowed to dry completely before application of the next to minimize sample spot size. Once dried, the plate was developed using hexane:ethyl acetate:acetic acid (80:20:2 v/v/v) and allowed to dry completely before being stained with 0.05% (w/v) primuline in acetone:MilliQ water (4:1 v/v). Lipids were visualized under 365 nm UV light and the retention factor (R_f) for each standard was calculated (where R_f is the distance between the standard and baseline divided by the distance between the solvent front and baseline). Synthetic OAHFA 18:1 (*n*-9, *cis*)/ ω -O-16:0 and OAHFA 18:1 (*n*-9, *cis*)/ ω -O-32:1 (*n*-7, *cis*) **2** typically showed R_f values between 0.35 and 0.5. The corresponding OAHFA-enriched region was scraped from the meibum lane (supplemental Fig. S1). OAHFAs were extracted from the silica gel by methyl *tert*-butyl ether-based biphasic lipid extraction (27). The process was repeated for up to 10 meibum samples and the resulting enriched-OAHFA extracts were combined. Enrichment of the meibum OAHFAs by this method was confirmed by MS (data not shown).

OAHFA derivatization

N-(4-aminomethylphenyl)pyridinium (AMPP) was used to derivatize synthetic and meibum OAHFAs using a commercially available kit, as previously described (28, 29). The 1-(3-(aminomethyl)-4-iodophenyl)pyridin-1-ium (4-I-AMPP) was used to prepare 4-I-AMPP-derivatized OAHFAs by the same procedure.

OAHFA synthesis

A detailed description of the synthesis and characterization of OAHFA 18:1 (*n*-9, *cis*)/ ω -O-32:1 (*n*-9, *cis*) **1** is described below. Synthesis and characterization of OAHFA 18:1 (*n*-9, *cis*)/ ω -O-32:1 (*n*-7, *cis*) **2** and 18:1 (*n*-9, *cis*)/ ω -O-32:1 (*n*-9, *trans*) **3** is provided within the supplemental information.

MS

For double bond position determination, negative ion mass spectra of OAHFAs from meibum were acquired on a modified Orbitrap Elite mass spectrometer (Thermo Fisher Scientific, San Jose, CA) equipped with a heated ESI source. Pooled meibum extract was diluted 100-fold in methanol spiked with 5 mM ammonium acetate and infused directly into the ion source at a rate of 10 $\mu\text{l}\cdot\text{min}^{-1}$. Typical source conditions were as follows: ionization spray voltage -3.6 kV, source temperature 45°C , transfer capillary temperature 275°C , and Slens RF level 65–70%. Nitrogen was used as the sheath, auxiliary, and sweep gas, while helium served as the bath gas. The instrument was modified to allow infusion of ozone from an external generator to the helium buffer gas, as described by Marshall et al. (26). A schematic of the modification is shown in supplemental Fig. S8. In a typical experiment, the flow rate of O_2 through the generator was set at ~ 0.2 $\text{l}\cdot\text{min}^{-1}$ with generator power output at 40% to obtain approximately 220 $\text{g}\cdot\text{Nm}^{-3}$ of ozone (or approximately 17% ozone in oxygen, w/w).

Collision-induced dissociation (CID) and ozone-induced dissociation (OzID) experiments were both conducted on mass-selected OAHFA $[\text{M}-\text{H}]^{-}$ species using an isolation width of 1.5 Th. CID experiments were performed at a normalized collision energy of 34 (arbitrary units) with a 30 ms activation time, while OzID was facilitated through an increased activation time (3 s) with a normalized collision energy of 0. All mass spectra represent the averaged acquisition of at least 50 scans, acquired at a resolution of 120,000 (at m/z 400). Mass calibration was performed in negative ion mode prior to analysis, providing a mass accuracy of <3 ppm. Double bond position was assigned based on characteristic neutral losses in OzID spectra. These neutral losses have previously been reported (30), but are provided for convenience in supplemental Table S1.

For determination of ester position within AMPP-derivatized OAHFAs, positive ion mass spectra were acquired on an LTQ Orbitrap XL (Thermo Fisher Scientific) equipped with an ESI source. AMPP-derivatized OAHFA in methanol with 5 mM ammonium acetate was infused into the source at a rate of 10 $\mu\text{l}\cdot\text{min}^{-1}$ and ionized under the following conditions: ionization spray voltage +4 kV, transfer capillary temperature 275°C , capillary voltage +11 V, and tube lens voltage +75 V. Nitrogen gas was used as the sheath, auxiliary, and sweep gas, while helium served as the bath gas. OAHFA $[\text{M}+\text{AMPP}]^{+}$ ions were mass selected with an isolation width of 1.0 Th. CID experiments were performed at a normalized collision energy of 45 (arbitrary units). Higher-energy C-trap dissociation experiments used a normalized collision energy of 60. The mass spectra shown represent a minimum acquisition of 50 scans obtained at a resolution of 70,000.

Photodissociation (PD) and radical-directed dissociation (RDD) experiments were performed on a linear ion-trap mass spectrometer (LTQ XL; Thermo Fisher Scientific) equipped with an ESI source. Typical source parameters were: spray voltage +4 kV and capillary temperature 250°C , with the following gas settings: sheath gas, 10; sweep gas, 2; and auxiliary gas, 8 (arbitrary units). Capillary and tube lens voltage were set at +50 V and +250 V, respectively. Nitrogen was used as the sheath, sweep, and auxiliary gas, while helium served as the bath gas. Ions were mass selected with a window of 1.5 Th and activated by either CID or PD. RDD was facilitated by an MS^3 sequence in which PD was performed followed by CID of the mass-selected radical cation formed in the PD event. The linear ion trap was modified to facilitate PD experiments, as previously described (31, 32). In brief, a quartz window was installed on the posterior plate of the vacuum housing to allow transmission of 266 nm laser pulses from a flashlamp-pumped Nd:YAG laser (Continuum, Santa Clara, CA). The laser beam (~ 30 $\text{mJ}\cdot\text{cm}^{-2}$) was directed into the trap via two right-angle bending prisms, which were adjusted to optimize beam alignment with the ion cloud.

RESULTS

Identification of OAHFAs in human meibum

Negative mode ESI allows partial fractionation of meibum lipids, as other more abundant classes (e.g., WEs and cholesterol esters) are not efficiently ionized in this modality. Negative ion ESI-MS of a crude lipid extract obtained from human meibum results in a series of abundant ions between m/z 700 and 800. Using a high resolution mass analyzer, the three most abundant $[\text{M}-\text{H}]^{-}$ anions appeared at m/z 729.7, 757.7, and 785.7, and were assigned to OAHFAs with sum compositions of 48:2, 50:2, and 52:2, respectively;

an observation consistent with prior literature (see supplemental Fig. S9) (9, 11, 33). Gas phase purification of the $[M-H]^-$ precursor ion corresponding to the most abundant OAHFA 50:2 was achieved by mass selection in a linear

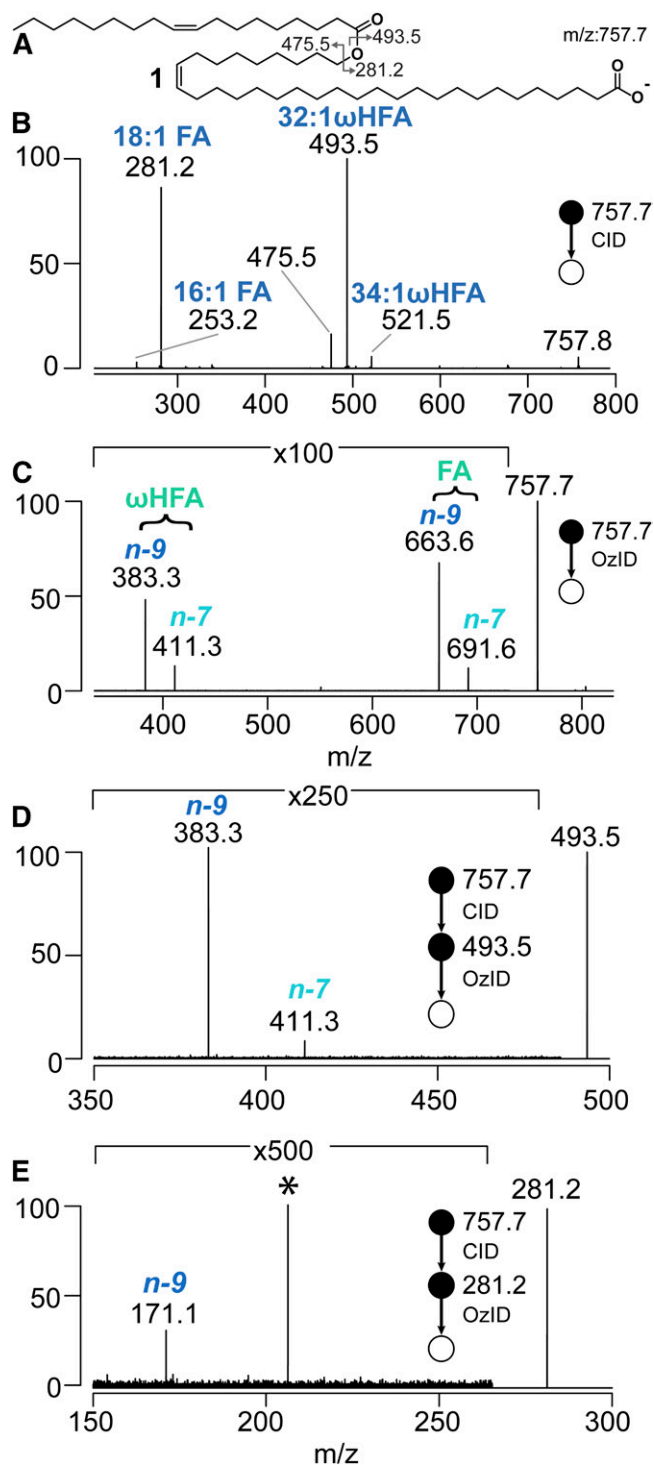


Fig. 1. A: Putative molecular structure of OAHFA 18:1/32:1 **1** derived from meibum. B: CID mass spectrum of m/z 757.7 precursor ion. C: The OzID mass spectrum of the m/z 757.7 precursor ion provided evidence for double bond positions at $n-9$ and $n-7$ locations in both HFA and FA. Sequential CID/OzID spectra identifying carbon-carbon double bond location in HFA 32:1 chain (D) and FA 18:1 chain (E). The * indicates an artifact signal in the spectrum.

ion trap mass spectrometer. Subsequent CID yielded the spectrum shown in **Fig. 1B**. Product ions in the CID spectrum provided evidence for the presence of at least two structural isomers. Ions at m/z 281.2, 475.5, and 493.5 were assigned as $[FA-H]^-$, $[HFA-H_2O]^-$, and $[HFA-H]^-$, respectively, and were consistent with a composition of OAHFA 18:1/32:1 (e.g., Fig. 1A). Less abundant $[FA-H]^-$ and $[HFA-H]^-$ ions observed at m/z 253.2 and 521.5 indicated the presence of a second minor isomer of the form OAHFA 16:1/34:1. While informative, these MS/MS data did not provide information on the position of the ester linkage or the sites and stereochemistry of unsaturation, and did not exclude the possibility of methyl chain-branching. Assumptions about each of these possible structural motifs led us to propose the putative structure **1** shown in Fig. 1A.

Assignment of double bond positions

Assigning the sites of unsaturation in long hydrocarbon chains using contemporary MS and nuclear magnetic resonance approaches is challenging. We have previously used gas-phase ozonolysis of mass-selected ions within ion-trap mass spectrometers to unequivocally assign carbon-carbon double bond position in a variety of lipids and natural products (34–36). The ion trap used in the present study was modified to perform OzID experiments (37). Mass selection and trapping of the $[M-H]^-$ anion derived from OAHFA 50:2 inside the mass spectrometer for 3 s in the presence of ozone resulted in the OzID spectrum shown in Fig. 1C. This spectrum displayed diagnostic ions at m/z 663.6 and 691.6, indicative of sites of unsaturation at the $n-9$ and $n-7$ positions in the FA chain (see supplemental Table S1) (30). Analogous ions at m/z 383.3 and 411.3 revealed both $n-9$ and $n-7$ double bonds in the HFA chain. While this agreed with previously reported unsaturation patterns for HFA 32:1 released upon saponification of meibum (38), the presence of isomeric OAHFA 16:1/34:1 (see above) prevented unambiguous assignment of unsaturation patterns to OAHFA 18:1/32:1 based on these findings alone. To overcome this, we performed sequential CID/OzID experiments involving mass selection of the m/z 757.7 precursor ion, CID to release the m/z 493.5 product ion corresponding to the HFA 32:1 chain, reisolated, and subsequent ozonolysis (Fig. 1D). An analogous CID/OzID spectrum targeting unsaturation in the FA 18:1 chain (m/z 281.2) is shown in Fig. 1E. The spectrum in Fig. 1D showed diagnostic ions confirming the presence of two isomeric HFA chains with double bonds at $n-9$ and $n-7$ (m/z 383.3 and 411.3, respectively), while similar interrogation of the FA 18:1 revealed only an $n-9$ isomer (m/z 171.1, Fig. 1E). Taken together, these data suggest the presence of two dominant regioisomeric OAHFAs in human meibum, namely, OAHFA 18:1($n-9$)/32:1($n-9$) **1** and OAHFA 18:1($n-9$)/32:1($n-7$) **2**. Analogous CID and OzID experiments were used to interrogate the structure of meibum-derived OAHFA 48:2 and 52:2 (see supplemental Figs. S10, S11). These data provide evidence for the presence of OAHFA 16:1($n-7$)/32:1($n-9$), OAHFA 16:1($n-7$)/32:1($n-7$), OAHFA 18:1($n-9$)/30:1($n-9$), OAHFA 18:1($n-9$)/30:1($n-7$), and

OAHFA 18:1(*n*-9)/34:1(*n*-9), with the possibility of other minor contributing isomers.

Assignment of ester regiochemistry

OAHFAs were previously assumed to be ω -esterified based on the putative structure of the HFA liberated upon saponification (38). However, the recent discovery that FAHFA lipids exhibit a diversity of regioisomeric esters (1) demands that the position of esterification in ultra-long chain naturally occurring OAHFAs be unequivocally determined. To interrogate meibum OAHFA ester position, we employed a charge-switch derivatization procedure using AMPP (28). This approach has been reported to afford up to 20-fold increases in mass spectral detection sensitivity when used with FAs. Furthermore, CID of mass-selected [FA+AMPP]⁺ ions can induce charge-remote fragmentation to provide additional structural details (29). To this end, an OAHFA-enriched fraction prepared from meibum using TLC was derivatized with AMPP. Positive ion ESI of the derivatized meibum fraction resulted in an abundant ion at *m/z* 925.8, corresponding to the [M+AMPP]⁺ cation of OAHFA 50:2. Isolation of this ion and activation by CID resulted in a spectrum dominated by a product ion at *m/z* 643.6 (supplemental Fig. S12), corresponding to the neutral loss of FA 18:1 (−282.3 Da) via the well-described charge-remote *cis*-elimination mechanism (26, 39). Reisolation of the *m/z* 643.6 product ion and subjecting it to further CID (i.e., MS³) gave rise to the spectrum shown in Fig. 2A. This spectrum exhibited a near complete profile of carbon-carbon bond fission along the hydrocarbon chain that was consistent with prior reports of charge-remote fragmentation in AMPP-derivatized FAs (29). Interruptions to this 14 Da peak spacing observed between *m/z* 519 and 545 can be ascribed to the unsaturation in HFA 32:1(*n*-9) and HFA 32:1(*n*-7) (see above); but more importantly, a stark 42 Da spacing was present between *m/z* 601.5 and the mass-selected precursor ion at *m/z* 643.6. Accurate mass determination showed this loss to be propene, providing direct evidence for the presence of a terminal alkene in the mass-selected HFA product ion. It follows that this terminal alkene motif can only be derived from the unimolecular dissociation of an ω -substituted OAHFA, as illustrated in Fig. 2A. The absence of other diagnostic peak spacings in the spectrum supports the conclusion that this substitution is exclusive. The 42 Da neutral loss pattern was repeated in the MS³ analysis of other OAHFAs present in meibum (e.g., OAHFA 48:2 and OAHFA 52:2, see supplemental Fig. S13). Taken together, these data overwhelmingly support the assignment of ω -substitution in the HFAs in OAHFAs (9) and appears to be a distinguishing feature, along with the ultra-long chain lengths, of this FAHFA subclass.

Investigation of possible methyl chain branching

The profiles of FAs and HFAs liberated by saponification of meibum (or its fractions) are known to include methyl-branched structures classified as *iso* (methyl-substitution at the penultimate carbon of the chain) or *anteiso* (methyl substitution on the third carbon counted from the methyl end of the chain) (21–23). While small amounts

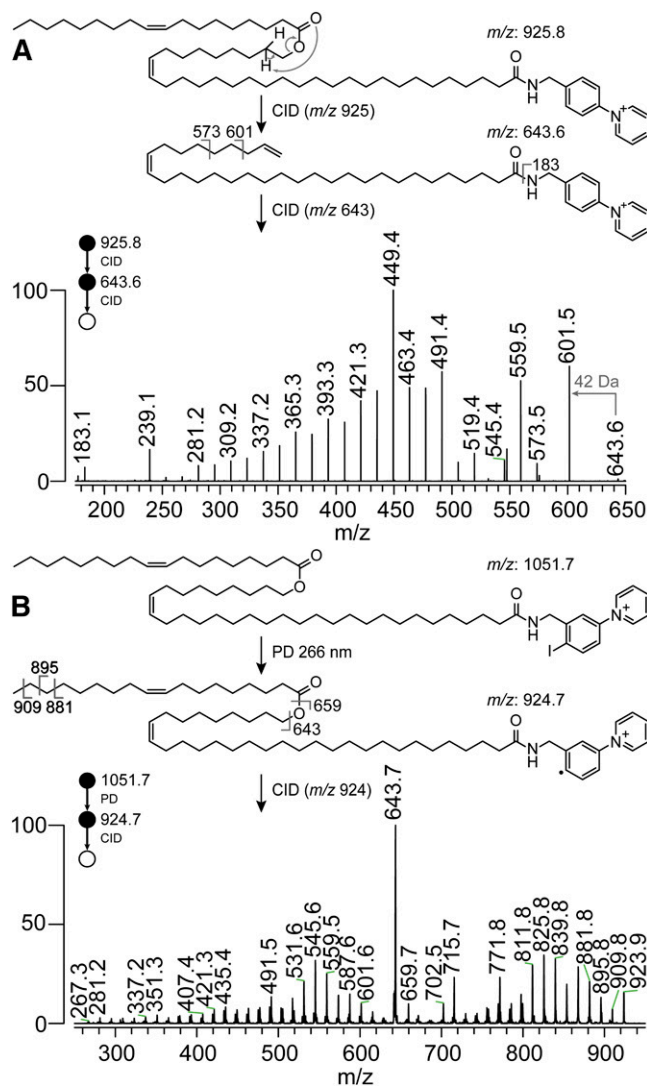


Fig. 2. A: MS³ spectrum of AMPP-derivatized meibum-derived OAHFA 18:1/32:1 shows a diagnostic neutral loss of 42 Da (*m/z* 601) indicative of the presence of a terminal alkene that can be directly ascribed to ω -substitution of the ester on the HFA backbone. B: RDD mass spectrum of 4-I-AMPP-derivatized meibum OAHFA 50:2 showed product ions resulting from carbon-carbon bond dissociation along the entire acyl chain length. The uninterrupted nature of this pattern is consistent with the absence of methyl branching. A straight-chain hydrocarbon structure was thus assigned to both FA and HFA portions of the molecule.

of *anteiso*-chain branching have been reported for HFAs in meibum (38), the spectrum in Fig. 2A shows no interruptions in the fragmentation pattern that would be diagnostic of chain branching in the HFA portion. Likewise, CID of the AMPP-derivatized OAHFAs did not yield analogous product ions for the FA chain in this structure, making it difficult to rule out the possibility of chain branching within this motif (e.g., supplemental Fig. S12B). An alternative derivatization strategy based on RDD has previously been deployed to specifically localize chain branching in lipids (32, 40). Following this strategy, an OAHFA-enriched TLC fraction from meibum was subjected to derivatization with the customized reagent, 4-I-AMPP, using the protocols reported for AMPP. Positive ion ESI of the

derivatized fraction produced an intense signal at m/z 1,051.7, corresponding to the modified OAHFA 50:2. Mass-selection of this precursor ion in a modified ion trap mass spectrometer facilitated irradiation of the ions with a single pulse from a 266 nm laser that drove prompt homolysis of the carbon-iodine bond and liberation of an $[M+AMPP]^{\bullet+}$ radical cation at m/z 924.7 (see supplemental Fig. S14). Mass-selection of the radical cation and subjecting it to CID yielded the RDD spectrum shown in Fig. 2B. The major RDD product ion observed at m/z 643.7 corresponded to dehydrated ω -HFA 32:1, similar to that observed for the AMPP derivative (compare Fig. 2A). The spectrum in Fig. 2B also exhibited an extensive series of product ions spaced 14 Da apart that represent dissociation of nearly every carbon-carbon bond along the entire 50-carbon length of the molecule. This exhaustive sequence coverage enabled careful investigation of any interruptions in product ion spacing that could result from methyl branching (40). In the absence of any 28 Da spacings in the RDD fragmentation pattern, the OAHFA 50:2 present in meibum was assigned, at least predominantly, to straight chain FA and HFA structures. RDD experiments performed on meibum-derived OAHFA 48:2 also showed no evidence for methyl chain branching (supplemental Fig. S15).

Total synthesis of OAHFAs

Taken together, these data suggest that the most abundant meibum OAHFA 50:2 exists predominately as two straight-chain isomers: OAHFA 18:1($n-9$)/ ω -O-32:1($n-9$) **1** and 18:1($n-9$)/ ω -O-32:1($n-7$) **2**. None of the experiments described thus far allowed de novo assignment of the configuration of the carbon-carbon double bonds, but it is well-known that unsaturated lipids present in animal tissues exist predominately as *cis* stereoisomers. Based on this assumption, OAHFA 18:1($n-9$, *cis*)/ ω -O-32:1($n-9$, *cis*) **1** and 18:1($n-9$, *cis*)/ ω -O-32:1($n-7$, *cis*) **2** were established as targets for total synthesis that could be used as standards to confirm all MS data to this point and resolve the remaining question of alkene stereochemistry. The strategy employed for the synthesis of OAHFA 18:1($n-9$, *cis*)/ ω -O-32:1($n-9$, *cis*) **1** is shown in **Scheme 1**.

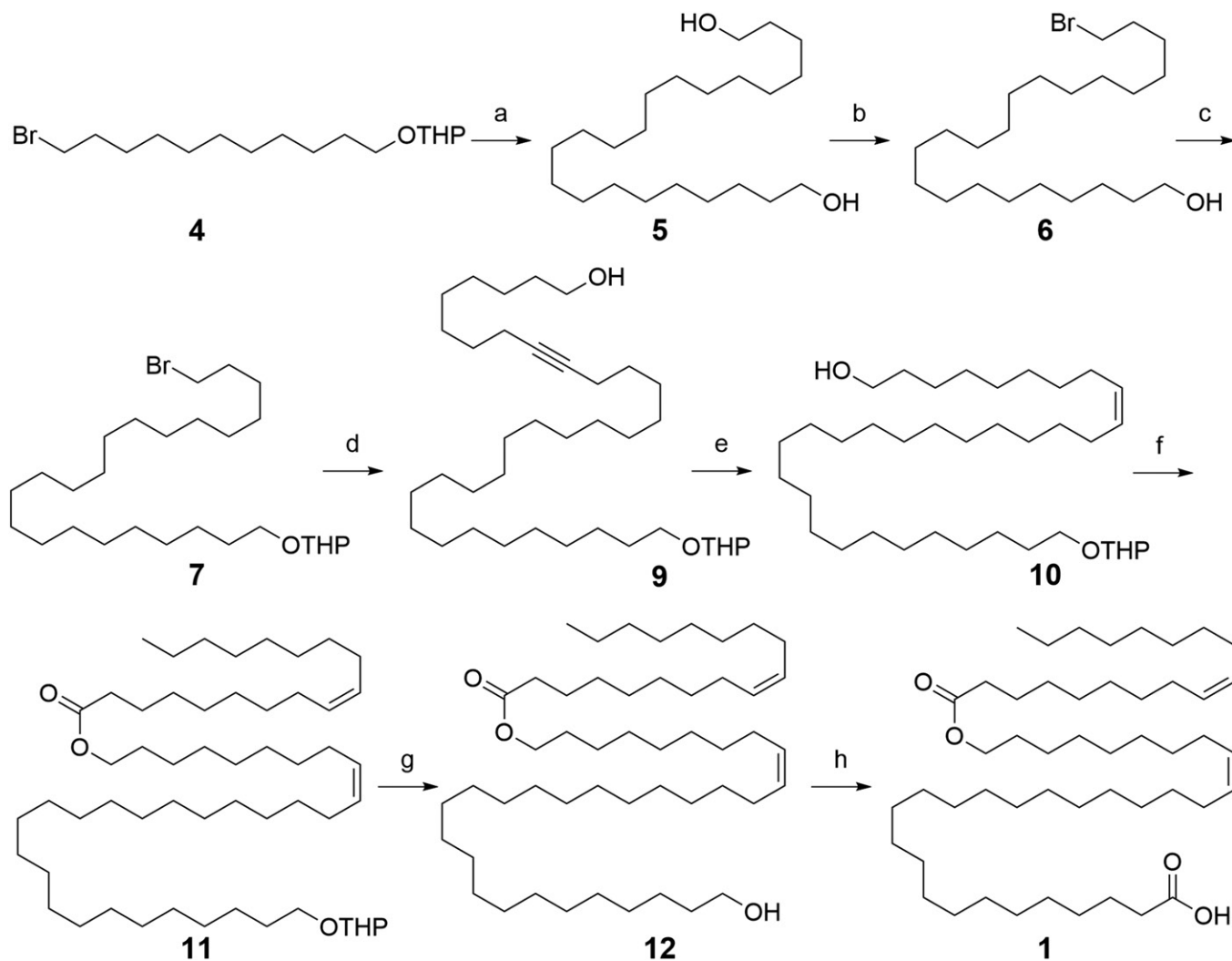
Retrosynthetic analysis suggested that the ω -O-32:1($n-9$, *cis*) portion of **1** could be accessed from key ω -alkynol intermediate **9**. The synthesis of **9** commenced with tetrahydropyran (THP)-protection of commercially available 11-bromoundecan-1-ol. Treatment of the alcohol with dihydropyran (DHP) in the presence of catalytic *p*-toluene sulfonic acid (TsOH) gave THP-ether **4** in 95% yield. Conversion of **4** to a Grignard reagent followed by homocoupling with a second equivalent of **4** using Li_2CuCl_4 (**41**) afforded the C22 bis-THP protected diol. Treatment of the crude intermediate product with TsOH in methanol at reflux afforded the deprotected diol **5** in 62% yield (over two steps) (**42**, **43**). Monobromination of **5** with HBr in cyclohexane gave bromoalkanol **6** (**44**) (69%), which was protected as THP-ether **7** (**45**) using DHP/TsOH in tetrahydrofuran (THF; 92%). The anion generated from tert-butyldimethylsilyl-protected dec-9-yn-1-ol **8** (**46**) with *n*-butyllithium in THF-hexamethylphosphoramide was

alkylated with **7** in the presence of tetrabutylammonium iodide at 50°C. The tert-butyldimethylsilyl deprotection of the crude with tetrabutylammonium fluoride afforded key intermediate **9** in 64% yield (over two steps). Partial hydrogenation of **9** using Lindlar catalyst and quinoline in benzene produced the (*Z*)-alkenol **10** in 98% yield. Oleic acid was coupled with **10** using dicyclohexylcarbodiimide and 4-dimethylaminopyridine in CH_2Cl_2 to give ester **11** (78%), which, upon treatment with camphorsulfonic acid in methanol-THF, afforded the penultimate alcohol **12** in 95% yield. Oxidation of **12** with Jones' reagent formed OAHFA 18:1($n-9$, *cis*)/ ω -O-32:1($n-9$, *cis*) **1** in 87% yield. Analogous procedures were employed using fragments with modified carbon chain lengths to synthesize OAHFA 18:1($n-9$, *cis*)/ ω -O-32:1($n-7$, *cis*) **2** (see supplemental Scheme S1).

When synthetic OAHFA standards 18:1($n-9$, *cis*)/ ω -O-32:1($n-9$, *cis*) **1** and 18:1($n-9$, *cis*)/ ω -O-32:1($n-7$, *cis*) **2** were subjected to the same suite of MS analyses as meibum-derived OAHFA 50:2, identical spectral signatures were observed, thus confirming: the locations of unsaturation (supplemental Figs. S16, S17); ester substitution (supplemental Fig. S18); and straight-chain structure (supplemental Fig. S19). However, the question of double bond geometry was still not resolved. A slight modification of the synthetic strategy wherein key intermediate **9** was reduced to the *trans* alkene (**22**, supplemental Scheme S2) before completing the synthesis as for **1**, afforded the mono-*trans* OAHFA 18:1($n-9$, *cis*)/ ω -O-32:1($n-9$, *trans*) **3**. OzID spectra were obtained across a range of reaction times for the synthetically derived geometrical isomers, OAHFA 18:1($n-9$, *cis*)/ ω -O-32:1($n-9$, *cis*) **1** and OAHFA 18:1($n-9$, *cis*)/ ω -O-32:1($n-9$, *trans*) **3** (see supplemental Fig. S20). Comparison of the OzID spectra revealed an appreciably greater abundance of ozonolysis product ions arising from the *cis/trans*-OAHFA **3** compared with the *cis/cis* **1**. More facile ozonolysis of *trans*-double bonds compared with *cis*-double bonds has been noted previously (**47**); but here, the comparison between the two sites of unsaturation within each lipid afforded a sensitive probe of double bond stereochemistry. The ratio of OzID product ions arising from the HFA (m/z 383) relative to the FA (m/z 663) were highly conserved for each isomer across all reaction times (see supplemental Fig. S20B). Between the stereoisomers, the peak intensity ratio was found to be significantly different with $I_{383}/I_{663} = 1.7 \pm 0.2$ compared with 0.9 ± 0.3 for the *cis/trans* and *cis/cis*-isomers, respectively. Equivalent experiments of meibum-derived OAHFA 50:2 returned a product ion ratio of 0.7 ± 0.3 in excellent agreement with the synthetic OAHFA 18:1($n-9$, *cis*)/ ω -O-32:1($n-9$, *cis*) **1**, thus confirming the *cis*-configuration of both HFA and FA double bonds in the naturally occurring lipid.

DISCUSSION

Herein, we have described complete structure elucidation and first total synthesis of OAHFAs. These unusual ultra-long chain lipids were first documented in meibomian gland secretions just over a decade ago (**8**), but have since



Scheme 1. Synthesis of OAHFA 18:1(*n*-9, *cis*)/ ω -O-32:1(*n*-9, *cis*) **1**. Reagents and conditions: a: (i) Mg, THF, 4 h, reflux then 4 in THF, Li_2CuCl_4 , -10°C to room temperature, 12 h; (ii) TsOH, methanol, reflux, 16 h, 62% (over two steps). b: HBr, cyclohexane, reflux, 6 h, 69%. c: DHP, TsOH, THF, 0°C to room temperature, 16 h, 92%. d: (step i) *tert*-butyl(dec-9-yn-1-yloxy)dimethylsilane **8**, *n*-butyllithium, THF-hexamethylphosphoramide, -78°C to -40°C , 1 h; **7** in THF, tetrabutylammonium iodide, -78°C to 60°C , 24 h; (step ii) tetrabutylammonium fluoride, THF, 0°C to room temperature, 12 h, 64% (for two steps). e: Lindlar catalyst, quinoline, benzene, room temperature, 12 h, 98%. f: Oleic acid, dicyclohexylcarbodiimide, 4-dimethylaminopyridine, CH_2Cl_2 , 0°C to room temperature, 24 h, 78%. g: CSA, methanol-THF, 0°C to room temperature, 12 h, 95%. h: Jones' reagent, acetone, room temperature, 1 h, 87% yielding the target **1**.


been detected in skin (5), equine sperm (6) and amniotic fluid (7), and as components of complex lipids, such as cholesteryl esters in meibum (14) and vernix caseosa (15) and acylceramides in the skin (i.e., esterified ω -hydroxyacyl-sphingosine) (5, 16–18). Since their first detection, the assignment of the hydroxy ester at the terminal (ω) position has largely resulted from early work using saponified meibum extractions (38); however, the more recent discovery of FAHFAs with multiple ester substitution positions has necessitated clarification of OAHFA structure. Additionally, the lipidomes in which OAHFAs are commonly found typically contain FAs with unusual double bond position and methyl-branched acyl chains: both important structural features could impart important functional aspects to OAHFAs.

The data we have presented within show that the most abundant meibum OAHFA 50:2 consists predominately of

two straight-chain isomers: OAHFA 18:1(*n*-9, *cis*)/ ω -O-32:1(*n*-9, *cis*) **1** and 18:1(*n*-9, *cis*)/ ω -O-32:1(*n*-7, *cis*) **2**. This largely agrees with prior work identifying key aspects of OAHFA components, such as FA by saponification of total meibum lipids. No studies currently exist exploring human meibum ω -HFA structure; however, we know from saponification of steer meibum lipids that 32:1 ω -HFAs exist predominately as either *n*-7 (~49%) or *n*-9 (~51%) (38). Our assignment of the FA in OAHFA 18:1/32:1 as 18:1(*n*-9) is in keeping with the dominant 18:1 FA isomer observed across other meibum lipids, such as cholesteryl and WES (21); however, small amounts of OAHFA 18:1(*n*-7)/32:1 could exist below our limit of detection. While many other lipids found in meibum contain substantial amounts of methyl-branched FA, we have determined that the majority of OAHFA 18:1/32:1 isomers in meibum exist as straight chain structures. Indeed, methyl-branching is uncommon

in monounsaturated acyl chains, but a small amount of *iso*-32:1 ω -HFA (0.4% of total ω -HFAs) has previously been reported in meibum (38), and \sim 1.3% of total meibum 18:1 FA is *iso*-branched (21). The lack of methyl-branching within OAHFA structure is important, as it likely affects lipid packing and molecular geometry (48, 49). This may be particularly important within the tear film lipid layer where OAHFAs are the dominant amphiphilic lipid (11, 13).

In the tear film, OAHFA structure can influence fluidity and packing in the lipid layer (48–50) and, consequently, tear film stability (51, 52). In the present work, we provide a detailed description of the synthesis of ultra-long chain biological analogs of OAHFAs, which will allow further research into the mode of action of these unique molecules in the various biological contexts in which they are found. Importantly, our reported synthetic strategy can be easily adapted to enable synthesis of OAHFAs complexed to other lipids, including cholesteryl esters and esterified ω -hydroxyacyl-sphingosine, allowing interrogation of their function in their resident lipidomes.

In summary, we have shown that the most abundant ultra-long chain OAHFA found in meibum, OAHFA 50:2, consists of two main isomers: 18:1 (*n*-9, *cis*)/ ω -O-32:1 (*n*-9, *cis*) **1** and 18:1 (*n*-9, *cis*)/ ω -O-32:1 (*n*-7, *cis*) **2**. The challenges posed in determining the full structure of OAHFAs (i.e., low abundance within a highly complex lipidome) were overcome using an integrated suite of advanced MS experiments that afforded sufficient information to guide the first total synthesis of ultra-long chain OAHFA natural products and, ultimately, confirmation of the lipid structure. More broadly, complete knowledge of OAHFA structure and development of flexible synthetic routes enabling access to key analogs (e.g., double bond regioisomers, saturated OAHFAs, and alkynyl derivatives) will motivate experiments to elucidate structure-function properties in their various biological contexts. 

The authors thank Prof. Thomas Millar and Dr. Burkhardt Schuett (Western Sydney University) for many helpful discussions. Dr. Alan MacCarone (University of Wollongong) is acknowledged for technical assistance.

REFERENCES

- Yore, M. M., I. Syed, P. M. Moraes-Vieira, T. Zhang, M. A. Herman, E. A. Homan, R. T. Patel, J. Lee, S. Chen, O. D. Peroni, et al. 2014. Discovery of a class of endogenous mammalian lipids with anti-diabetic and anti-inflammatory effects. *Cell*. **159**: 318–332.
- Nelson, A. T., M. J. Kolar, Q. Chu, I. Syed, B. B. Kahn, A. Saghatelian, and D. Siegel. 2017. Stereochemistry of endogenous palmitic acid ester of 9-hydroxystearic acid and relevance of absolute configuration to regulation. *J. Am. Chem. Soc.* **139**: 4943–4947.
- Lee, J., P. M. Moraes-Vieira, A. Castoldi, P. Aryal, E. U. Yee, C. Vickers, O. Parnas, C. J. Donaldson, A. Saghatelian, and B. B. Kahn. 2016. Branched fatty acid esters of hydroxy fatty acids (FAHFAs) protect against colitis by regulating gut innate and adaptive immune responses. *J. Biol. Chem.* **291**: 22207–22217.
- Moraes-Vieira, P. M., A. Saghatelian, and B. B. Kahn. 2016. GLUT4 expression in adipocytes regulates de novo lipogenesis and levels of a novel class of lipids with antidiabetic and anti-inflammatory effects. *Diabetes*. **65**: 1808–1815.
- Hirabayashi, T., T. Anjo, A. Kaneko, Y. Senoo, A. Shibata, H. Takama, K. Yokoyama, Y. Nishito, T. Ono, C. Taya, et al. 2017. PNPLA1 has a crucial role in skin barrier function by directing acylceramide biosynthesis. *Nat. Commun.* **8**: 14609.
- Wood, P. L., K. Scoggin, B. A. Ball, M. H. Troedsson, and E. L. Squires. 2016. Lipidomics of equine sperm and seminal plasma: Identification of amphiphilic (O-acyl)- ω -hydroxy-fatty acids. *Theriogenology*. **86**: 1212–1221.
- Wood, P. L., B. A. Ball, K. Scoggin, M. H. Troedsson, and E. L. Squires. 2018. Lipidomics of equine amniotic fluid: Identification of amphiphilic (O-acyl)- ω -hydroxy-fatty acids. *Theriogenology*. **105**: 120–125.
- Butovich, I. A., E. Uchiyama, and J. P. McCulley. 2007. Lipids of human meibum: mass-spectrometric analysis and structural elucidation. *J. Lipid Res.* **48**: 2220–2235.
- Butovich, I. A., J. C. Wojtowicz, and M. Molai. 2009. Human tear film and meibum. Very long chain wax esters and (O-acyl)- ω -hydroxy fatty acids of meibum. *J. Lipid Res.* **50**: 2471–2485.
- Butovich, I. A., H. Lu, A. McMahon, and J. C. Eule. 2012. Toward an animal model of the human tear film: biochemical comparison of the mouse, canine, rabbit, and human meibomian lipidomes. *Invest. Ophthalmol. Vis. Sci.* **53**: 6881–6896.
- Brown, S. H. J., C. M. E. Kunnen, E. Duchoslav, N. K. Dolla, M. J. Kelso, E. B. Pappas, P. Lazon de la Jara, M. D. P. Willcox, S. J. Blanksby, and T. W. Mitchell. 2013. A comparison of patient matched meibum and tear lipidomes. *Invest. Ophthalmol. Vis. Sci.* **54**: 7417–7424.
- Schuett, B. S., and T. J. Millar. 2013. An investigation of the likely role of (O-acyl) ω -hydroxy fatty acids in meibomian lipid films using (O-oleyl) ω -hydroxy palmitic acid as a model. *Exp. Eye Res.* **115**: 57–64.
- Butovich, I. A. 2013. Tear film lipids. *Exp. Eye Res.* **117**: 4–27.
- Butovich, I. A. 2009. Cholesteryl esters as a depot for very long chain fatty acids in human meibum. *J. Lipid Res.* **50**: 501–513.
- Kalužíková, A., V. Vrkošlav, E. Harazim, M. Hoskovec, R. Plavka, M. Buděšínský, Z. Bosáková, and J. Cvačka. 2017. Cholesteryl esters of ω -(O-acyl)-hydroxy fatty acids in vernix caseosa. *J. Lipid Res.* **58**: 1579–1590.
- řKindt, R., L. Jorge, E. Dumont, P. Couturon, F. David, P. Sandra, and K. Sandra. 2012. Profiling and characterizing skin ceramides using reversed-phase liquid chromatography-quadrupole time-of-flight mass spectrometry. *Anal. Chem.* **84**: 403–411.
- McMahon, A., I. A. Butovich, N. L. Mata, M. Klein, R. Ritter, J. Richardson, D. G. Birch, A. O. Edwards, and W. Kedzierski. 2007. Retinal pathology and skin barrier defect in mice carrying a Stargardt disease-3 mutation in elongase of very long chain fatty acids-4. *Mol. Vis.* **13**: 258–272.
- Vasireddy, V., Y. Uchida, N. Salem, S. Y. Kim, M. N. A. Mandal, G. B. Reddy, R. Bodepudi, N. L. Alderson, J. C. Brown, H. Hama, et al. 2007. Loss of functional ELOVL4 depletes very long-chain fatty acids (\geq C28) and the unique ω -O-acylceramides in skin leading to neonatal death. *Hum. Mol. Genet.* **16**: 471–482.
- Rissmann, R., H. W. W. Groenink, A. M. Weerheim, S. B. Hoath, M. Ponc, and J. A. Bouwstra. 2006. New insights into ultrastructure, lipid composition and organization of vernix caseosa. *J. Invest. Dermatol.* **126**: 1823–1833.
- Sadowski, T., C. Klose, M. J. Gerl, A. Wójcik-Maciejowicz, R. Herzog, K. Simons, A. Reich, and M. A. Surma. 2017. Large-scale human skin lipidomics by quantitative, high-throughput shotgun mass spectrometry. *Sci. Rep.* **7**: 43761.
- Nicolaides, N., J. K. Kaitaranta, T. N. Rawdah, J. I. Macy, F. M. Boswell, and R. E. Smith. 1981. Meibomian gland studies: comparison of steer and human lipids. *Invest. Ophthalmol. Vis. Sci.* **20**: 522–536.
- Ansari, M. N. A., H. C. Fu, and N. Nicolaides. 1970. Fatty acids of the alkane diol diesters of vernix caseosa. *Lipids*. **5**: 279–282.
- Nicolaides, N., H. C. Fu, M. N. A. Ansari, and G. R. Rice. 1972. The fatty acids of wax esters and sterol esters from vernix caseosa and from human skin surface lipid. *Lipids*. **7**: 506–517.
- Hancock, S. E., B. L. J. Poad, A. Batarseh, S. K. Abbott, and T. W. Mitchell. 2017. Advances and unresolved challenges in the structural characterization of isomeric lipids. *Anal. Biochem.* **524**: 45–55.
- Liebisch, G., J. A. Vizcaíno, H. Köfeler, M. Trötzmüller, W. J. Griffiths, G. Schmitz, F. Spener, and M. J. O. Wakelam. 2013. Shorthand notation for lipid structures derived from mass spectrometry. *J. Lipid Res.* **54**: 1523–1530.
- Marshall, D. L., J. T. Saville, A. T. MacCarone, R. Ailuri, M. J. Kelso, T. W. Mitchell, and S. J. Blanksby. 2016. Determination of ester position in isomeric (O-acyl)-hydroxy fatty acids by ion trap mass spectrometry. *Rapid Commun. Mass Spectrom.* **30**: 2351–2359.

27. Matyash, V., G. Liebisch, T. V. Kurzchalia, A. Shevchenko, and D. Schwudke. 2008. Lipid extraction by methyl-tert-butyl ether for high-throughput lipidomics. *J. Lipid Res.* **49**: 1137–1146.
28. Bollinger, J. G., W. Thompson, Y. Lai, R. C. Oslund, T. S. Hallstrand, M. Sadilek, F. Turecek, and M. H. Gelb. 2010. Improved sensitivity mass spectrometric detection of eicosanoids by charge reversal derivatization. *Anal. Chem.* **82**: 6790–6796.
29. Yang, K., B. G. Dilthey, and R. W. Gross. 2013. Identification and quantitation of fatty acid double bond positional isomers: a shotgun lipidomics approach using charge-switch derivatization. *Anal. Chem.* **85**: 9742–9750.
30. Brown, S. H. J., T. W. Mitchell, and S. J. Blanksby. 2011. Analysis of unsaturated lipids by ozone-induced dissociation. *Biochim. Biophys. Acta.* **1811**: 807–817.
31. Ly, T., B. B. Kirk, P. I. Hettiarachchi, B. L. J. Poad, A. J. Trevitt, G. da Silva, and S. J. Blanksby. 2011. Reactions of simple and peptidic alpha-carboxylate radical anions with dioxygen in the gas phase. *Phys. Chem. Chem. Phys.* **13**: 16314–16323.
32. Pham, H. T., T. Ly, A. J. Trevitt, T. W. Mitchell, and S. J. Blanksby. 2012. Differentiation of complex lipid isomers by radical-directed dissociation mass spectrometry. *Anal. Chem.* **84**: 7525–7532.
33. Chen, J., K. B. Green-Church, and K. K. Nichols. 2010. Shotgun lipidomic analysis of human meibomian gland secretions with electrospray ionization tandem mass spectrometry. *Invest. Ophthalmol. Vis. Sci.* **51**: 6220–6231.
34. Wang, H., D. N. Leach, M. C. Thomas, S. J. Blanksby, P. I. Forster, and P. G. Waterman. 2011. Bisresorcinol derivatives from *Grevillea glauca*. *Helv. Chim. Acta.* **94**: 1812–1819.
35. Shou, Q., L. K. Banbury, A. T. Maccarone, D. E. Renshaw, H. Mon, S. Griesser, H. J. Griesser, S. J. Blanksby, J. E. Smith, and H. Wohlmut. 2014. Antibacterial anthranilic acid derivatives from *Geijera parviflora*. *Fitoterapia.* **93**: 62–66.
36. Thomas, M. C., T. W. Mitchell, D. G. Harman, J. M. Deeley, J. R. Nealon, and S. J. Blanksby. 2008. Ozone-induced dissociation: elucidation of double bond position within mass-selected lipid ions. *Anal. Chem.* **80**: 303–311.
37. Marshall, D. L., H. T. Pham, M. Bhujel, J. S. R. Chin, J. Y. Yew, K. Mori, T. W. Mitchell, and S. J. Blanksby. 2016. Sequential collision- and ozone-induced dissociation enables assignment of relative acyl chain position in triacylglycerols. *Anal. Chem.* **88**: 2685–2692.
38. Nicolaides, N., E. C. Santos, and K. Papadakis. 1984. Double-bond patterns of fatty acids and alcohols in steer and human meibomian gland lipids. *Lipids.* **19**: 264–277.
39. Dua, S., J. H. Bowie, S. Dua, B. A. Cerda, and C. Wesdemiotis. 1998. The facile loss of formic acid from an anion system in which the charged and reacting centres cannot interact. *Chem. Commun. (Camb.)* **0**: 183–184.
40. Pham, H. T., A. J. Trevitt, T. W. Mitchell, and S. J. Blanksby. 2013. Rapid differentiation of isomeric lipids by photodissociation mass spectrometry of fatty acid derivatives. *Rapid Commun. Mass Spectrom.* **27**: 805–815.
41. Tamura, M., and J. Kochi. 1971. Coupling of Grignard reagents with organic halides. *Synthesis.* **1971**: 303–305.
42. Roy, R. K., E. B. Gowd, and S. Ramakrishnan. 2012. Periodically grafted amphiphilic copolymers: nonionic analogues of ionenes. *Macromolecules.* **45**: 3063–3069.
43. Drescher, S., A. Meister, A. Blume, G. Karlsson, M. Almgren, and B. Dobner. 2007. General synthesis and aggregation behaviour of a series of single-chain 1,omega-bis(phosphocholines). *Chemistry.* **13**: 5300–5307.
44. Greaves, J., K. R. Munro, S. C. Davidson, M. Riviere, J. Wojno, T. K. Smith, N. C. O. Tomkinson, and L. H. Chamberlain. 2017. Molecular basis of fatty acid selectivity in the zDHHC family of S-acyltransferases revealed by click chemistry. *Proc. Natl. Acad. Sci. USA.* **114**: E1365–E1374.
45. Paiva, D., T. Markowski, B. Dobner, G. Brezesinski, H. Möhwald, M. do Carmo Pereira, and S. Rocha. 2015. Synthesis and study of the complex formation of a cationic alkyl-chain bola amino alcohol with DNA: in vitro transfection efficiency. *Colloid Polym. Sci.* **293**: 3167–3175.
46. Sandtorv, A. H., and H-R. Bjørsvik. 2015. Scope and mechanistic limitations of a Sonogashira coupling reaction on an imidazole backbone. *Eur. J. Org. Chem.* **2015**: 4658–4666.
47. Poad, B. L. J., H. T. Pham, M. C. Thomas, J. R. Nealon, J. L. Campbell, T. W. Mitchell, and S. J. Blanksby. 2010. Ozone-induced dissociation on a modified tandem linear ion-trap: observations of different reactivity for isomeric lipids. *J. Am. Soc. Mass Spectrom.* **21**: 1989–1999.
48. Rilfors, L. 1985. Difference in packing properties between iso and anteiso methyl-branched fatty acids as revealed by incorporation into the membrane lipids of *Acholeplasma laidlawii* strain A. *Biochim. Biophys. Acta.* **813**: 151–160.
49. Lim, J. B., and J. B. Klauda. 2011. Lipid chain branching at the iso- and anteiso-positions in complex chlamydia membranes: a molecular dynamics study. *Biochim. Biophys. Acta.* **1808**: 323–331.
50. Zhang, Y-M., and C. O. Rock. 2008. Membrane lipid homeostasis in bacteria. *Nat. Rev. Microbiol.* **6**: 222–233.
51. Bron, A. J., J. M. Tiffany, S. M. Gouveia, N. Yokoi, and L. W. Voon. 2004. Functional aspects of the tear film lipid layer. *Exp. Eye Res.* **78**: 347–360.
52. McCulley, J. P., and W. E. Shine. 2001. The lipid layer: the outer surface of the ocular surface tear film. *Biosci. Rep.* **21**: 407–418.